Proceedings of the ASME 2010 International Design Engineering Technical Conferences & Computers and Information in Engineering Conference
IDETC/CIE 2010
August 15-18, 2010, Montreal, Quebec, Canada

DRAFT-DETC2010-28049

BALANCING ENERGY TO ESTIMATE DAMPING IN A FORCED OSCILLATOR WITH COMPLIANT CONTAFCT

Jin-Wei Liang
Department of Mechanical Engineering
Ming Chi University of Technology, Taipei, TAIWAN

Brian Feeny
Department of Mechanical Engineering
Michigan State University, Michigan, USA

ABSTRACT

This work identifies damping parameters from compliant-contact vibration systems using energy dissipation concept. To develop the identification algorithms, the energy loss as registered in the force-displacement relationship of the real system is balanced against that of a theoretical model incorporating with an idealized compliant contact. Two approaches, including one based on the harmonic response assumption and the other directly integrating the system responses, are developed. Numerical investigations are performed to illustrate the reliability of the identification algorithms.

INTRODUCTION

Friction and damping estimation is of great importance to the design, analysis, control, and stability prediction of machines, cutting tools, vehicles and structures [1], some of which can be very sensitive to the damping model [2-8]. Damping estimation can be done by force measurement [9-11], damping coefficient estimation, or general parameter estimation [12].

Long established vibration properties can be exploited for damping estimation in free-response and forced-response systems with viscous damping or Coulomb damping only. Here, we continue a line of work on extracting Coulomb and viscous friction parameters from free oscillation decrements [13-15], and then forced oscillations by which analytical solutions [16-18] are used to obtain estimation equations [19]. Limitations are that these methods are not applicable for damping which is not "small," they rely on analytical solutions of single-degree-of-freedom linear systems, and they do not treat friction models other than Coulomb and viscous (see for example, references [8, 20-26]). As such, energy balancing is potentially more generally applicable [27]. There are ways to extend energy balancing to the estimation of damping in multi-degree-of-freedom systems, as well [28-31].

In the previous energy-balance work, energy loss in the real vibration systems was expressed in terms of a theoretical model consisting of, for example, viscous and Coulomb friction, and balanced against the input energy. The identification algorithms were derived either by assuming the system with harmonic input and output motion or by directly integrating the input and output signals. These studies concentrate on the rigidly grounded, or rigid-contact problems, such as Coulomb and viscous [27,29], and viscous and quadratic [30].

In this paper, we apply the energy-dissipation identification idea to compliant-contact problems. Many researchers have reported compliance in friction contacts [2-10, 25]. Contact compliance is sufficiently prevalent that a viable damping estimation tool would be of value. This paper aims to add a method to the set of tools for handling these problems. To derive the identification algorithms, the energy dissipated in the theoretical compliant model is introduced in the next section.

OSCILLATOR WITH AN IDEAL COMPLIANT CONTACT

Contact compliance could be caused by the asperity deformations at the contact interfaces or by the elastic deformation of the surrounding structures. A schematic diagram which shows a base-excited, dual-damped oscillator with an ideal massless compliant contact is presented in Figure 1, where $x(t)$ and $y(t)$ indicate the displacements of sliding mass and base excitation, $z(t)$ denotes the displacement of the hypothetical contact surface, K_z represents the stiffness of the contact joint, and $f(t)$ models the friction force, which is implicitly time dependent via dependence on $x(t)$, $\dot{x}(t)$, $y(t)$, and $z(t)$.

The system shown in Figure 1 can have response that consists of "macroscopic slipping" and "microsticking" phases [23]. A schematic $f-\dot{x}$ diagram is presented in Figure 2 in which both the macroscopic sliding phase (between points D, A and B, C) and the microsticking phase (between points C, D and A, B) are illustrated. We assume that the friction force is modeled as Coulomb friction with equal static and kinetic friction

coefficients. Hence, the following equation of motion can be used during sliding:

$$m\ddot{x} + c\dot{x} + kx + F_k \,\mathrm{sgn}(\dot{x}) = kY\cos\omega t \quad (1)$$

where F_k is the magnitude of the friction force.

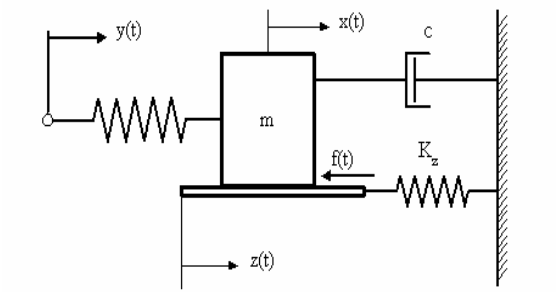

Fig. 1 A schematic diagram showing a forced-compliant oscillator with an idealized massless contact.

During the slipping phase, the ideal contact surface is motionless, such that $\dot{z}(t) = \mathbf{0}$. The slipping motion continues until a direction reversal, at which time microsticking begins at time t_1. Once the microsticking phase commences, the model changes to

$$m\ddot{x} + c\dot{x} + kx + K_z z(t) = kY\cos\omega t \quad (2)$$

$$z(t) = Z_m \,\mathrm{sgn}(\dot{x}(t_1^-)) + x(t) - X_t \quad (3)$$

in which Z_m (a positive number equal to F_k / K_z) is the maximum deflection of the contact, and X_t (a value with a sign) is the displacement of the mass before microsticking starts. If X_m denotes the maximum displacement of the sliding mass (a positive number), then $X_t = \pm X_m$. Note that the motions of the sliding mass and contact surface are identical during the microsticking interval, such that $\dot{x}(t) = \dot{z}(t)$. This feature can be observed in Eq. (3). The microsticking motion gives way to slip when the magnitude of the restoring force $K_z Z(t)$ is greater than the friction force F_k. At that moment, the next half cycle of motion begins.

In what follows, the energy dissipated by the dual-damped oscillator, with compliant contact, subjected to harmonic base excitations is formulated.

ENERGY BALANCE WITH A COMPLIANT CONTACT

A typical force-velocity relationship of an idealized massless compliant-contact model with a constant sliding friction coefficient is shown in Figure 2, in which the hysteretic structure represents the microsticking phenomenon that occurs during the velocity reversals [23]. In Figure 2, points C, D, A, B and time instants t_1, t_s, t_2, t_r correspond to the onsets of forward microstick, forward slip, backward microstick and backward slip, respectively.

Accommodating such a compliant-contact model, the analytical energy loss, W_d, that would be dissipated during one forcing cycle can be expressed as

$$W_d = \int_{t_1}^{t_2} f(t)\dot{x}\,\mathrm{sgn}(\dot{x})dt + \int_{t_2}^{t_1+T} f(t)\dot{x}\,\mathrm{sgn}(\dot{x})dt + \int_{t_1}^{t_1+T} c\dot{x}\dot{x}dt. \quad (4)$$

Assuming a symmetric response, the first and second integrals are equal. For the case in which the sliding friction is constant, the stored contact-spring energy between times t_1 and t_s, in the first integral of equation (4), is returned between times t_2 and t_r in the second integral. As such

$$W_d = 2\int_{t_s}^{t_2} F_k \dot{x}\,\mathrm{sgn}(\dot{x})dt + \int_{t_1}^{t_1+T} c\dot{x}\dot{x}dt = 2\int_{t_r}^{t_1+T} F_k \dot{x}\,\mathrm{sgn}(\dot{x})dt + \int_{t_1}^{t_1+T} c\dot{x}\dot{x}dt$$

The dissipated energy is balanced against the applied input energy, $W_a = \int_{t_1}^{t_1+T} ky(t)\dot{x}dt$, such that te energy balance for the compliant oscillator during one cycle is $W_d = W_a$ [23], or

$$W_d = 2\int_{t_s}^{t_2} F_k \dot{x}\,\mathrm{sgn}(\dot{x})dt + \int_{t_1}^{t_1+T} c\dot{x}\dot{x}dt$$

$$= 2\int_{t_r}^{t_1+T} F_k \dot{x}\,\mathrm{sgn}(\dot{x})dt + \int_{t_1}^{t_1+T} c\dot{x}\dot{x}dt = W_a = \int_{t_1}^{t_1+T} ky(t)\dot{x}dt \quad (5)$$

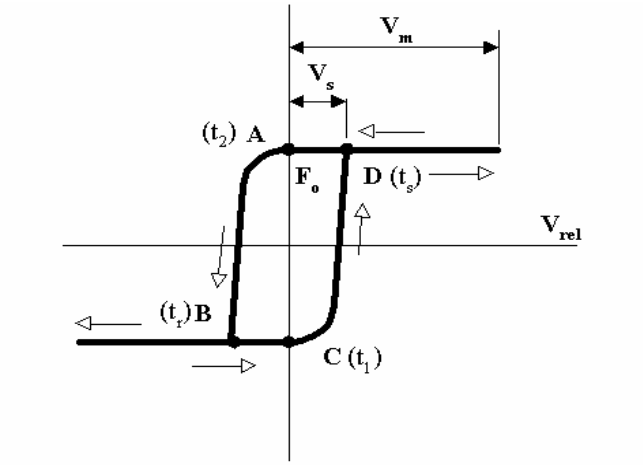

Fig. 2 A schematic diagram showing the $f - \dot{x}$ relationship of the sliding mass with a compliant contact model subjected to harmonic excitations.

Previous research [27,29,30] suggests that it is more simple and accurate to use numerical integrals of equation (5), from sampled time histories of $y(t)$ and $\dot{x}(t)$, than to use analytical expressions derived from a harmonic response assumption. However, the harmonic-motion formulation can be insightful regarding the roles of amplitude, phase, and frequency in the identification, sensitivities of identified parameters, and may also be useful for implementation in some cases. In addition, features of the system response subjected to harmonic excitations also resemble harmonic functions [23]. Thus, we will develop the identification scheme based on both simple integration of signals, and the harmonic-response assumption.

THE DIRECT INTEGRATION APPROACH

The energy-balance identification process for the complaint vibration systems can be implemented by directly integrating

the input and response data numerically. The energy balance of equation (5) can be written for several input/output responses, $y_i(t)$ and $\dot{x}_i(t)$, $i = 1,\ldots, n$, as

$$a_i F_k + b_i c = W_{ai} \tag{6}$$

where

$$a_i = 2\int_{t_s}^{t_2} \dot{x}_i \,\mathrm{sgn}(\dot{x}_i)dt \tag{7a}$$

$$b_i = \int_{t_1}^{t_1+T} \dot{x}_i^2(t)dt\,. \tag{7b}$$

Given n = 2 independent steady-state input/output pairs, $y_i(t)$, $\dot{x}_i(t)$ and $y_j(t)$, $\dot{x}_j(t)$, equation (6) represents two independent equations in two unknowns, F_k and c, which can be solved to produce the following identification equations:

$$\tilde{F}^{\bullet}_{kij} = \frac{b_j W_{di} - b_i W_{dj}}{\Delta} \tag{8a}$$

$$\tilde{c}^{\bullet}_{ij} = \frac{a_i W_{dj} - a_j W_{di}}{\Delta} \tag{8b}$$

where $\Delta = a_i b_j - a_j b_i$. Note that the parameters a and b have their counterparts in our previous study of rigid-contact problems [27]. However, due to the effects of contact compliance, the upper and lower limits of integration of parameter "a" are different from those of [27].

Given multiple steady-state responses, and hence multiple equations in (6), the parameters F_k and c can be estimated by a least-squares solution. That is, if a set of n equations (6) is written in matrix form as

$$\underline{A}\,\underline{p} = \underline{w}$$

where $\underline{p} = [F_k \quad c]^T$, $\underline{w} = [W_{a1} \quad W_{a2} \quad \ldots \quad W_{an}]^T$, and $\underline{A}$ is a matrix of coefficients

$$\underline{A} = \begin{bmatrix} a_1 & b_1 \\ \vdots & \vdots \\ a_n & b_n \end{bmatrix}.$$

The least squares solution is thus

$$\underline{p} = (\underline{A}^T \underline{A})^{-1} \underline{A}^T \underline{w}\,. \tag{9}$$

Given an estimate of F_k, and measurements of $X_{\max}$ or $X_{\min}$ and X_s or X_r, we can estimate the contact stiffness as

$$K_z = (X_{\max} - X_r)/F_k = -(X_{\min} - X_s)/F_k\,. \tag{10}$$

ENERGY BALANCE BASED ON A HARMONIC-RESPONSE ASSUMPTION

Assuming that $x(t) \cong X\cos(\omega t - \phi)$ and letting $t_1 = \phi/\omega + \pi/\omega$, we manipulate Eq. (5) to acquire

$$\begin{aligned} W_d &= 2F_k X(1 - \cos(\omega t_s - \phi)) + c\pi\omega X^2 \\ &= 2F_k X(1 + \cos(\omega t_r - \phi)) + c\pi\omega X^2 \end{aligned} \tag{11}$$

or

$$\begin{aligned} W_d &= 2F_k X(1 + \sqrt{(\omega X)^2 - V_s^2}\,/\,\omega X) + c\pi\omega X^2 \\ &= 2F_k X(1 + \sqrt{(\omega X)^2 - V_r^2}\,/\,\omega X) + c\pi\omega X^2 \end{aligned} \tag{12}$$

or finally

$$W_d = 2F_k(X - X_s) + c\pi\omega X^2 = 2F_k(X + X_r) + c\pi\omega X^2 \tag{13}$$

where V_s, t_s, and X_s are the velocity, time, and displacement corresponding to the forward-slip transition, and V_r, t_r, and X_r are the velocity, time, and displacement corresponding to the reverse-slip transition [23]. Note that $X_s < \mathbf{0}$ and $X_r > \mathbf{0}$ in equation (8), such that positive quantities add up. In the limit of a rigid contact, $t_s \to t_1 = \phi/\omega + \pi/\omega$, and $t_r \to t_2 = \phi/\omega$. Inserting into equation (11),

$$W_d \to 2F_k X(1 - \cos\pi) + c\pi\omega X^2 = 4F_k X + c\pi\omega X^2$$

from the t_s limit, and likewise from the t_r limit, which is consistent with energy dissipated from a rigid contact [27].

Furthermore, with the harmonic assumption, the applied energy per cycle is

$$W_a = \pi k Y X \sin\phi \tag{14}$$

Either Equation (11), (12) or (13) can be equated with equation (14) in implementing the estimation process, depending on whether V_s, t_s, or X_s is more accessible. The algorithms derived based upon Equations (11)-(13) will be designated as the compliant harmonic-response approach since the harmonic-response approximation has been made.

Thus, if Eq. (13) is applied as the identification crux, after equating W_d in (13) to W_a in (14) with two sets of input/output data, the following estimation equations (for F_k and c) can be obtained:

$$\tilde{F}^{\Delta}_{k12} = \frac{\pi k(Y_1 X_1 X_2^2 \sin\phi_1 - Y_2 X_1^2 X_2 \sin\phi_2)}{2(q_1 X_2^2 - q_2 X_1^2)}, \tag{15a}$$

$$\tilde{c}^{\Delta}_{12} = \frac{k(q_1 Y_2 X_2 \sin\phi_2 - q_2 Y_1 X_1 \sin\phi_1)}{\omega(q_1 X_2^2 - q_2 X_1^2)}, \tag{15b}$$

where $q_1 = X_1 - X_{1s}$ and $q_2 = X_2 - X_{2s}$, (which can be defined likewise based on the reverse slip transition, $q_i = X_i + X_{ir}$), and where the subscripts "1, 2" denote two different excitation levels and responses at the same frequency. Unless the system possesses strong nonlinearity, the phase angles between input and output corresponding to different excitation levels at the same frequency can be assumed to be the

same. Therefore, $\phi_1 \cong \phi_2 = \phi$, which leads to the following approximate identification equations.

$$\tilde{F}_{k12}^{\Delta} = \frac{\pi k X_1 X_2 \sin\phi (Y_1 X_2 - Y_2 X_1)}{2(q_1 X_2^2 - q_2 X_1^2)} \tag{16a}$$

$$\tilde{c}_{12}^{\Delta} = \frac{k \sin\phi (q_1 Y_2 X_2 - q_2 Y_1 X_1)}{\omega (q_1 X_2^2 - q_2 X_1^2)}. \tag{16b}$$

Equations (16) describe the identification algorithms of the compliant harmonic-response approach based on the forward (or backward) slip displacement, X_s (or X_r). Hence, we will further denote Equations (16) as the compliant harmonic-response-X_s approach hereafter. Meanwhile, the superscript "Δ" is adopted to designate this perspective.

In fact, X_s (or X_r) is not the only choice as the identification crux. For example, if t_s, the time instant corresponding to the forward slip is utilized as the identification crux, the following identifying equation for F_k can be obtained

$$\tilde{F}_{k12}^{*} = \frac{\pi k (Y_1 X_2 \sin\phi_1 - Y_2 X_1 \sin\phi_2)}{2\left[X_2 (1+\cos\omega t_{s1}) - X_1 (1+\cos\omega t_{s2})\right]} \tag{17}$$

where t_{s1} and t_{s2} indicate the time instants at which the forward-slip events (that associate with two individual excitation levels at the same frequency) take place. Again, if the system possess weak nonlinearity, it may be reasonable to apply a simplifying approximation $t_{s1} \cong t_{s2} = t_s$, and $\phi_1 \cong \phi_2 = \phi$. To this end, equation (18) can be further simplified, and the two-point identification equations are

$$\tilde{F}_{k12}^{*} = \frac{\pi k \sin\phi (Y_1 X_2 - Y_2 X_1)}{2(1+\cos\omega t_s)(X_2 - X_1)} \tag{18a}$$

$$\tilde{c}_{12}^{*} = \frac{k \sin\phi (Y_1 - Y_2)}{\omega (X_1 - X_2)} \tag{18b}$$

The algorithms depicted in Equations (18) and superscripted with "$*$" are denoted as the compliant harmonic-response-t_s approach.

Alternatively, if we adopt the forward-slip velocity, V_s, as the identification crux, the following pair of identification equations is obtained

$$\tilde{F}_{k12}^{\circ} = \frac{\pi k \omega X_1 X_2 \sin\phi (Y_1 X_2 - Y_2 X_1)}{2(\alpha_1 X_2^2 - \alpha_2 X_1^2)}, \tag{19a}$$

$$\tilde{c}_{12}^{\circ} = \frac{k \sin\phi (\alpha_1 Y_2 X_2 - \alpha_2 Y_1 X_1)}{\omega (\alpha_1 X_2^2 - \alpha_2 X_1^2)}. \tag{19b}$$

where $\alpha_1 = \omega X_1 + \sqrt{(\omega X_1)^2 - V_{s1}^2}$ and $\alpha_2 = \omega X_2 + \sqrt{(\omega X_2)^2 - V_{s2}^2}$. The algorithms presented in Equations (19) are denoted as the compliant harmonic-response-V_s approach and superscripted using "$\circ$".

Based on the derivations, the new identification methods are divided into the compliant harmonic-response-X_s, -t_s, and -V_s approaches, depending on whether X_s, t_s, or V_s is applied. In the next section, we will validate these compliant energy-balance methods with numerical examples. By investigating the numerical systems with known parameters, insights of these identification methods can be acquired, and the effectiveness of the methods are revealed.

NUMERICAL INVESTIGATIONS

To conduct the numerical simulations, we adopted the following system parameters: $m = 2.42$ kg, $c = 90.0$ N-sec/m, $k = 2310$ N/m, $K_z = 208000$ N/m, $F_k = 1.28$ N ($\zeta = 0.602$). In order to understand the sensitivity of estimation accuracy on the excitation frequency, three different excitation frequencies were applied. They are $\omega_1 = 4.92$ Hz, $\omega_2 = 3.5$ Hz, and $\omega_3 = 11.1$ Hz. Among these frequencies, ω_1 is equal to the undamped natural frequency of the system.

Table 1 shows the input/output amplitudes, the forward-slip displacement, X_{is}, velocity, V_{is}, time instant, t_{is}, and the phase angles (between the input and output signal), ϕ_i, corresponding to $\omega_1 = 4.92$ Hz, where the subscript "i" denotes different excitation levels. To illustrate the process which we apply to estimate X_{is}, V_{is}, and X_i listed in Table 1, we plot the acceleration-displacement and acceleration-velocity relationships in Figure 3. In Figure 3(b), a steeply sloped straight-line structure appears, which depicts the microsticking transition between two macroscopic sliding phases. This microsticking transition is, in fact, a special compliant-contact feature and can be used to estimate X_i and X_{is}. In the same simulation, another compliant-contact feature, emerging as a curved transition associated with a corner structure, is presented in the acceleration-velocity plot, Figure 3(d). The corner structure in the acceleration-velocity plot corresponds to the forward-slip onset velocity, V_{is}. While it is not shown here, quantities t_{is} and ϕ_i were determined using time-domain signals, in which t_s was determined by examining the time instant right after the abrupt jumps appearing in the acceleration time trace [23], and ϕ_i was determined by measuring the time difference between corresponding "zero crossings" occurred in the input and output displacement signals.

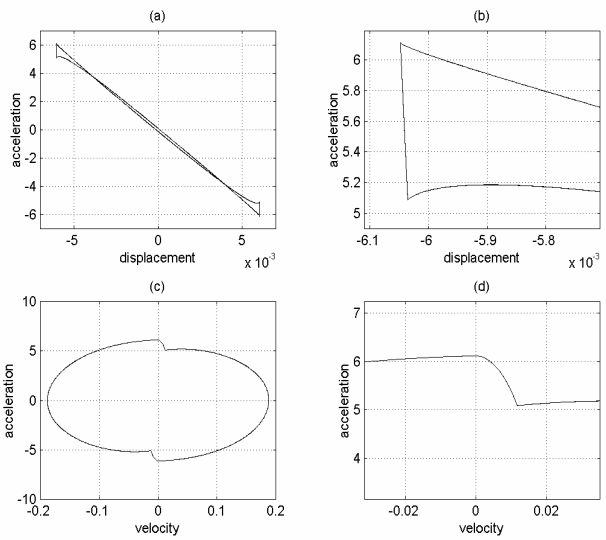

Figure 3: Simulation of the forced compliant oscillator ($\omega_1 = 4.92$ Hz), numerical versions of (a) the acceleration-displacement plot, (b) zoom-in detail of the acceleration-displacement plot, (c) the acceleration-velocity plot, and (d) zoom-in detail of the acceleration-velocity plot.

Table 1: The input/output amplitudes and the motion-related quantities required in implementing the compliant harmonic-response identification process ($\omega_1 = 4.92$ Hz).

Y_i (m)	X_i (m)	X_{is} (m)	V_{is} (m/s)	ϕ_i (rad)	t_{is} (sec)
0.004	0.00273	-0.00272	0.00774	1.522	2.9E-3
0.006	0.00439	-0.00438	0.00995	1.536	2.3E-3
0.008	0.00605	-0.00604	0.01175	1.550	2.0E-3
0.010	0.00771	-0.00770	0.01330	1.552	1.7E-3
0.012	0.00937	-0.00936	0.01470	1.552	1.6E-3

Table 2: The numerical integration data and the damping estimates obtained from the system by direct integration of the energies from the signals. Pair-wise damping estimations are also shown.

Y_i	a_i	b_i
0.004	$a_1 = 0.010885625$	$b_1 = 0.00072729$
0.006	$a_2 = 0.017525003$	$b_2 = 0.00187708$
0.008	$a_3 = 0.024164700$	$b_3 = 0.00356234$
0.010	$a_4 = 0.030804807$	$b_4 = 0.00578304$
0.012	$a_5 = 0.037445013$	$b_5 = 0.00853919$

$\tilde{\tilde{c}}^{\bullet}_{ij}$	W_{di}	$\tilde{\tilde{F}}^{\bullet}_{kij}$
$\tilde{\tilde{c}}^{\bullet}_{12} = 90.0134$	$W_{d1} = 0.07939719$	$\tilde{\tilde{F}}^{\bullet}_{k12} = 1.279799$
$\tilde{\tilde{c}}^{\bullet}_{23} = 90.0114$	$W_{d2} = 0.19139123$	$\tilde{\tilde{F}}^{\bullet}_{k23} = 1.280015$
$\tilde{\tilde{c}}^{\bullet}_{34} = 90.0113$	$W_{d3} = 0.35158214$	$\tilde{\tilde{F}}^{\bullet}_{k34} = 1.280030$
$\tilde{\tilde{c}}^{\bullet}_{45} = 90.0115$	$W_{d4} = 0.55996992$	$\tilde{\tilde{F}}^{\bullet}_{k45} = 1.280003$
$\tilde{\tilde{c}}^{\bullet}_{15} = 90.0119$	$W_{d5} = 0.81655453$	$\tilde{\tilde{F}}^{\bullet}_{k15} = 1.279901$

Table 3: The pair-wise estimates of damping parameters of the numerical simulating system ($\omega_1 = 4.92$ Hz, $c = 90.0$ N-sec/m, $\tilde{\tilde{F}}_k = 1.28$ N) obtained from the compliant harmonic-response- t_s approach (denoted as $\tilde{\tilde{F}}^{*}_{kij}$ and $\tilde{\tilde{c}}^{*}_{ij}$), the compliant harmonic-response- X_s approach (denoted as $\tilde{\tilde{F}}^{\Delta}_{kij}$ and $\tilde{\tilde{c}}^{\Delta}_{ij}$) and the compliant harmonic-response- V_s approach (denoted as $\tilde{\tilde{F}}^{\circ}_{kij}$ and $\tilde{\tilde{c}}^{\circ}_{ij}$).

$\tilde{\tilde{F}}^{*}_{kij}$ (N)	$\tilde{\tilde{c}}^{*}_{ij}$ (N-sec/m)	$\tilde{\tilde{c}}^{\Delta}_{ij}$ (N-sec/m)
$\tilde{\tilde{F}}^{*}_{k12} = 1.291$	$\tilde{\tilde{c}}^{*}_{12} = 90.05$	$\tilde{\tilde{c}}^{\Delta}_{12} = 90.02$
$\tilde{\tilde{F}}^{*}_{k23} = 1.297$	$\tilde{\tilde{c}}^{*}_{23} = 89.99$	$\tilde{\tilde{c}}^{\Delta}_{23} = 89.98$
$\tilde{\tilde{F}}^{*}_{k34} = 1.297$	$\tilde{\tilde{c}}^{*}_{34} = 89.99$	$\tilde{\tilde{c}}^{\Delta}_{34} = 89.99$
$\tilde{\tilde{F}}^{*}_{k45} = 1.297$	$\tilde{\tilde{c}}^{*}_{45} = 89.99$	$\tilde{\tilde{c}}^{\Delta}_{45} = 89.99$
$\tilde{\tilde{F}}^{*}_{k15} = 1.294$	$\tilde{\tilde{c}}^{*}_{15} = 90.01$	$\tilde{\tilde{c}}^{\Delta}_{15} = 89.99$
$\tilde{\tilde{F}}^{\Delta}_{kij}$ (N)	$\tilde{\tilde{F}}^{\circ}_{kij}$ (N)	$\tilde{\tilde{c}}^{\circ}_{ij}$ (N-sec/m)
$\tilde{\tilde{F}}^{\Delta}_{k12} = 1.295$	$\tilde{\tilde{F}}^{\circ}_{k12} = 1.286$	$\tilde{\tilde{c}}^{\circ}_{12} = 90.071$
$\tilde{\tilde{F}}^{\Delta}_{k23} = 1.299$	$\tilde{\tilde{F}}^{\circ}_{k23} = 1.293$	$\tilde{\tilde{c}}^{\circ}_{23} = 90.004$
$\tilde{\tilde{F}}^{\Delta}_{k34} = 1.298$	$\tilde{\tilde{F}}^{\circ}_{k34} = 1.293$	$\tilde{\tilde{c}}^{\circ}_{34} = 90.000$
$\tilde{\tilde{F}}^{\Delta}_{k45} = 1.298$	$\tilde{\tilde{F}}^{\circ}_{k45} = 1.294$	$\tilde{\tilde{c}}^{\circ}_{45} = 89.997$
$\tilde{\tilde{F}}^{\Delta}_{k15} = 1.297$	$\tilde{\tilde{F}}^{\circ}_{k15} = 1.289$	$\tilde{\tilde{c}}^{\circ}_{15} = 90.018$

ESTIMATION BASED ON DIRECT INTEGRATION OF MEASURED SIGNALS

The integration data from equation (7) and damping estimates obtained from the energy balance of equation (6) are presented in Table 2. The integrations of energies were performed with Simpson's rule. The least-squares solution based on the displayed data yields estimates $\tilde{\tilde{c}}^{\bullet}_{LS} = 90.0115$ Ns/m and $\tilde{\tilde{F}}^{\bullet}_{kLS} = 1.279987$ N. The root mean squared residual, normalized by the vector $\underline{w}$, was $\underline{r}$ = 9.1587e-07. The superscript " $\bullet$ " indicates the estimates obtained from the direct-integration approach. These estimates can be directly compared to those in obtained later by the harmonic response assumption. Table 2 also shows the pair-wise estimates based on equations (8). The means of the pair-wise estimates are $\tilde{\tilde{c}}^{\bullet}_{mean} = 90.0119$ Ns/m and $\tilde{\tilde{F}}^{\bullet}_{kmean} = 1.279950$ N, with corresponding standard deviations of 0.00087 and 0.000098.

ESTIMATION BASED ON THE HARMONIC-RESPONSE APPROXIMATION

The least squares approximations were obtained from the values of Table 1 using sets of five balances of equations (11)-(13) and (14) for each of the X_s, $-t_s$, and $-V_s$ perspectives, also using the individual (not averaged) values of t_s and ϕ. The resulting estimations were $\tilde{c}_{LS}^{\Delta} = 90.0402$ Ns/m and $\tilde{F}_{kLS}^{\Delta} = 1.284786$ N with a normalized residual of 5.03e-05 for the X_s perspective, $\tilde{c}_{LS}^{*} = 90.0396$ Ns/m and $\tilde{F}_{kLS}^{*} = 1.285022$ N with a normalized residual of 4.98e-05 for the t_s perspective, and $\tilde{c}_{LS}^{\circ} = 90.0392$ Ns/m and $\tilde{F}_{kLS}^{\circ} = 1.285163$ N with a normalized residual of 4.97e-05 for the V_s perspective. The superscripts "Δ", "$*$"and "$\circ$" denote the compliant harmonic-response-X_s, $-t_s$ and $-V_s$ approaches, respectively.

Table 3 presents the estimated results separately obtained from the compliant harmonic-response-X_s, $-t_s$, and $-V_s$ approximations by using the data listed in Table 1, and the mean values of $t_{savg} = 2.1\times10^{-3}$ and $\phi_{avg} = 1.542$. In Table 3 all of the damping estimates are close to the known data regardless of the excitation level is high or low. The largest estimation error of dry-friction force in the same table is less than 1.5% among three different methods, whereas the largest estimation error of viscous damping is less than 0.1%.

In order to understand how the new identification algorithms perform in the off-resonance conditions, we simulated the systems with $\omega_2 = 3.5$ Hz and $\omega_3 = 11.1$ Hz. While not shown here, the estimation accuracies of these two cases degraded. For instance, the highest estimation error, in the $\omega_3 = 11.1$ Hz case, was more than 70% which is unacceptable.

DISCUSSION AND CONCLUSIONS

Through comparison, we find that the accuracy of the direct-integration approach is better than that of the compliant harmonic-response approaches. A similar trend has also been observed in our previous studies on the rigid-contact problems [27, 29, 30]. However, harmonic-response assumption also produced acceptable estimations. Assumptions used in least-squares and two-point harmonic approximations include the single harmonic. The two-point identification equations made use of a mean t_s and mean ϕ approximations, while the least squares solutions used individual t_s and ϕ values. Estimation results were similar.

This paper demonstrates the estimation of damping parameters from compliant-contact vibratory systems. An energy balance was applied in two ways, namely by using expressions based on a harmonic-response approximation, and by direct numerical integration of the measured response signals. These methods were developed based on the same ideas that have been applied in previous investigations on rigid-contact vibratory problems [27]. The characterization of transition properties such as the velocity, displacement, and time instant of the onsets of forward and backward stick and slip associated with the compliant-contact system are involved in the implementation of the identification methods. According to the investigations, we find that the contact compliance will not hinder the applicability of the estimation methods when modeling details are accommodated.

Moreover, as with other studies, it is found that the harmonic-response method works nicely when the system is excited near resonance. The estimation accuracy, however, degrades when the off-resonance excitations are met. The direct-integration approach provides better accuracy in the numerical examples. In implementation, the identification algorithms dealing with the compliant-contact problems involve more modeling details which in turn mandate more effort than with the rigid-contact model. Nonetheless, estimation of damping in the compliant-contact model is certainly feasible with the energy-balance approach.

REFERENCES

[1]. R. A. Ibrahim. Friction-induced vibration, chatter, squeal, and chaos: part ii-dynamics and modeling. Applied Mechanics Reviews, 47(7):227–255, 1994.

[2]. J. H. Griffin. Friction damping of resonant stresses in gas turbine engine airfoils. Journal of Engineering for Power, 102:329–333, 1980.

[3]. J.-H. Wang. Design of a friction damper to control vibration of turbine blades. In F. Pfeiffer A. Guran and K. Popp, editors, Dynamics and Friction: Modeling, Analysis, and Experiment. World Scientific, Singapore, 1996.

[4]. Y. Wang. An analytical solution for periodic response of elastic-friction damped systems. Journal of Sound and Vibration, 189(3):299–313, 1996.

[5]. J. Guillen and C. Pierre. Analysis of the forced response of dry-friction damped structural systems using and efficient hybrid frequency-time method. In Nonlinear Dynamics and Controls, volume ASME DE-Vol. 91, pages 41–50, 1996.

[6]. K. Y. Sanliturk and D. J. Ewins. Modeling two-dimensional friction contact and its application using harmonic balance method. Journal of Sound and Vibration, 193(2):511–524, 1996.

[7]. A. A. Ferri and B. S. Heck. Vibration analysis of dry damped turbine blades using singular perturbation theory. Journal of Vibration and Acoustics, 120(2):588–595, 1998.

[8]. A. J. McMillan, 1997, "A non-linear friction model for self-excited vibrations," *Journal of Sound and Vibration* 205 (3) 323-335.

[9]. S. Filippi, A. Akay, A. May, and M. M. Gola. Measurement of tangential contact hysteresis during microslip. Journal of Tribology-Transactions of the ASME, 126(3):482–489, 2004.

[10]. K.-H. Koh, J. H. Griffin, S. Filippi, and A. Akay, 2005, Characterization of Turbine Blade Friction Dampers,

Journal of Engineering for Gas Turbines and Power Volume 127, Issue 4, 856-862.
[11]. R. A. Ibrahim, Madhavan S., S. L. Qiao, and W. K. Chang. Experimental investigation of friction-induced noise in disc brake systems. International Journal of Vehicle Design, 23(3-4):218–240, 2000.
[12]. J. Beck and K. Arnold. Parameter Identification in Engineering and Science. John Wiley and Sons, New York, 1977.
[13]. A.Watari. Kikai-rikigaku. Kyouritsu (publisher), Tokyo, 1969.
[14]. B. F. Feeny and J.W. Liang. A decrement method for the simultaneous estimation of Coulomb and viscous friction. Journal of Sound and Vibration, 195(1):149–154., 1996.
[15]. J.-W. Liang and B. F. Feeny. Identifying Coulomb and viscous friction from free-vibration decrements. Nonlinear Dynamics, 16:337–347, 1998.
[16]. Den Hartog, J. P., 1931, "Forced vibration with combined Coulomb and viscous damping." *Transactions of the American Society of Mechanical Engineering*, 53 107-115.
[17]. Hundal, M. S., 1979, "Response of a base excited system with Coulomb and viscous friction." *Journal of Sound and Vibration*, 64, 371-378.
[18]. Shaw, S. W., 1986, "On the dynamic response of a system with dry friction." *Journal of Sound and Vibration*, 108(2) 305-325.
[19]. Liang, J.-W. and Feeny, B. F., 2004, "Identifying Coulomb and viscous friction in forced dual-damped oscillators," Journal of Vibration and Acoustics 126(1) 118-125.
[20]. Ibrahim, R. A., 1994, "Friction-induced vibration, chatter, squeal, and chaos: part I-mechanics of friction," *Applied Mechanics Reviews* 47, 209-226.
[21]. Armstrong-Helouvry, B., Dunpont, P., and Canudas De Wit, C., 1994, "A Survey of Models, Analysis Tools and Compensation Methods for the Control of Machines with Friction," *Automatica*, 30(7) pp.1083-1138.
[22]. Oden, J. T. and Martins, J. A. C., 1985, "Models and Computational Methods for Dynamic Friction Phenomena," *Comput. Mech. Appl. Mech. Eng.* 52(1-3) pp.527-634.
[23]. Liang, J. W. and Feeny, B. F., 1998, "Dynamical friction behavior in a forced oscillator with a compliant contact." *Journal of Applied Mechanics*, 65(1), 1998, 250-257.
[24]. Hinrichs, N., Oestreich, M., and Popp, K., 1998, "On the modeling of friction oscillator," *Journal of Sound and Vibration*, 216(3), 435-459
[25]. Haessig, D. A. and Friedland, B., 1991, "On the modeling and simulation of friction," *Journal of Dynamic Systems, Measurement and Control*, Vol. 113, 354-362.
[26]. H. Dankowicz, On the Modeling of Dynamic Friction Phenomena, *Zeitschrift fuer angewandte Mathematik und Mechanik* 79(6) (1999), 399-409.
[27]. Liang, J.-W. and Feeny, B. F., 2006, "Balancing energy to estimate damping parameters in forced oscillators," Journal of Sound and Vibration 295 (3-5) 988-998.
[28]. Tomlinson, G. R. and Hibbert, J. H., 1979, "Identification of the dynamic characteristics of a structure with Coulomb friction," Journal of Sound and Vibration, 64(2):233–242, 1979.
[29]. Liang, J.-W., 2007, "Damping estimation via energy-dissipation method," Journal of Sound and Vibration 307 (1-2) 349-364.
[30]. B. F. Feeny, 2007, "Estimating damping parameters in multi-degree-of-freedom vibration systems by balancing energy," In Proceedings of the 2007 ASME International Design Engineering Technical Conferences, pages DVD–ROM paper VIB–35340, Las Vegas, September 4-7.
[31]. B. F. Feeny, 2009, "Estimating damping parameters in multi-degree-of-freedom vibration systems by balancing energy," Journal of Vibration and Acoustics, 131 (4) 041005.
[32]. Prandina, M., Mottershead, J. E., and Bonisoli, E., 2009, "Damping identification in multiple degree-of-freedom systems using an energy balance approach," Journal of Physics: Conference Series 181(2009) 012006.